Chapter – VIII

Effect of Surface Roughness on the Lubrication Characteristics of Slider Bearing with an Exponential Film Profile: Rabinowitsch Fluid Model

8.1 Introduction

Recently, the study of the effect of surface roughness on the hydrodynamic lubrication of various bearing systems has attracted the attention of several researchers. This is mainly because; in practice all bearing surfaces are rough. The aspect ratio and absolute height of the asperities and valleys observed under the microscope vary greatly, depending on the material properties and on the method of surface preparation, height of the surface roughness may range from 0.05μm of les on polished surfaces to 10 μm on medium mechanical surfaces. Even the chemical degradation of the lubricants leading to the contamination lubricants is also one of the reasons for developing roughness on the bearing surface in some cases. Several methods have been proposed to study the effect of surface roughness on the bearing performance. The stochastic study of Tzeng and Saibel (1967) has fascinated several investigators in the field of Tribology. Christensen and Tonder (1973) used the stochastic concept to analyze the influence of transverse and longitudinal roughness on the steady state behaviour of journal bearings.While Elrod (1977) employed the perturbation technique to study the effect of surface roughness. Christensen and Tonder (1969, 1971. 1972) presented a comprehensive general analysis for the two types of one dimensional surface roughness patterns viz. longitudinal and transverse, based on the general probability density function and this approach formed the basis for the study of surface roughness effected by several researchers, Gururajan, K. and Prakash, (2003), Letalleur,.(2002), Lin,, Hsu, and Lai. (2002) and Lin,(1996). It is also found that, effect of surface roughness depends on the lubrication conditions. This has lead to the researchers (Etsion and Burstein, (1996), Etsion (2004), Dobrica *et.al.*2010, Tala-

Ighil *et.al.*(2011)) to investigate the effect of adding carefully controlled pictures of micro features in to the bearing surfaces.

Recently, the steady state performance of rough inclined stepped composite non-porous and porous slider bearings with micro polar fluids have been analyzed by Naduvinamani and Siddangouda (2010) and Siddangouda (2012) respectively. The effect of surface roughness and non-Newtonian micro polar fluids on dynamic characteristics of wide plane slider bearings by Lin *et. al.*(2013). Apart from these, Rabinowitsch fluid model is one of the fluid models which can be applied to analyze the non-linear behaviour of non-Newtonian lubricants.

Rabinowitsch fluid model is one of the models to establish the non-linear relationship between the shearing stress and shearing strain rate which can be described for one dimensional fluid flow as given in equation (2.1.1). The advantage of this model lies in the fact that the theoretical analysis for present model was verified with experimental justification by Wada and Hayashi (1971). In this chapter, an attempt has been made to study the effect of surface roughness and non-Newtonian Rabinowitsch fluid on the static characteristics of slider bearing with exponential film profile. On the basis of the stochastic the theory of Christensen (1969-70), a stochastic non-Newtonian Reynolds equation is derived. Analytical expressions of the steady load carrying capacity, pressure and frictional force are obtained. The results are in good agreement with smooth case.

8.2 Mathematical formulation of the problem

Figure 8.1 shows the physical geometry of exponential slider bearing with surface roughness on the lower bearing surface and the length of the curved part is L. Fluid in the film region is taken as non-Newtonian Rabinowitsch fluid. The lower bearing surface is moving with a velocity U in the x –direction.

Under the usual assumptions of hydrodynamic lubrication theory, equations of continuity and motion in Cartesian co-ordinates reduces to

$$\frac{\partial u}{\partial x}+\frac{\partial v}{\partial y}=0, \tag{8.2.1}$$

$$\frac{\partial \tau_{xy}}{\partial y}=\frac{\partial p}{\partial x}, \tag{8.2.2}$$

$$\frac{\partial p}{\partial y}=0, \tag{8.2.3}$$

where u and v are velocity components in x and y directions, p denotes the fluid film pressure.

The relevant boundary conditions for the velocity components are

i) At the upper surface $y = H$,

$$u=0,\ v=0; \tag{8.2.4}$$

ii) At the lower surface $y=0$,

$$u=U,\ v=0\ . \tag{8.2.5}$$

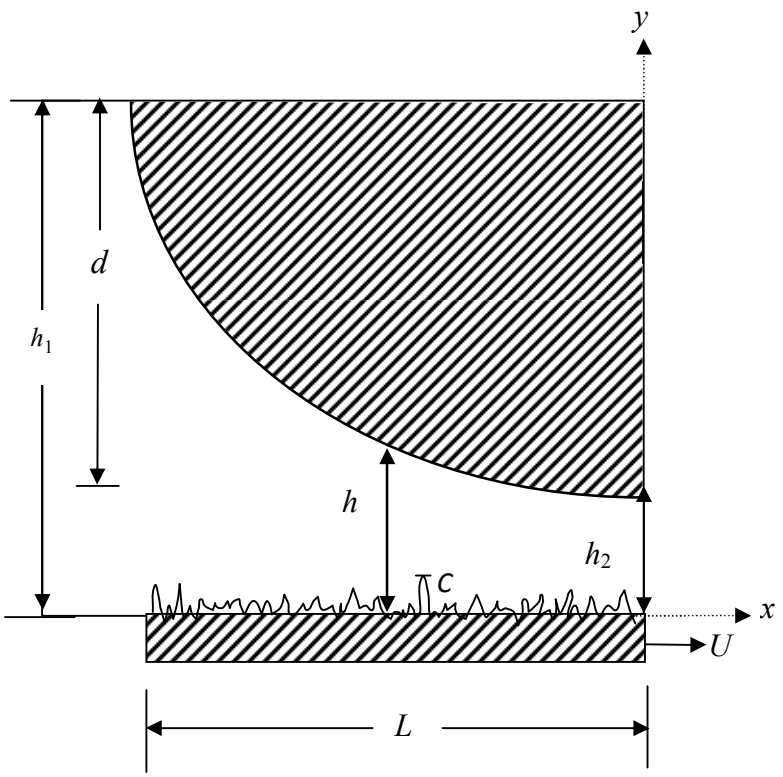

Figure 8.1 Physical Geometry of Exponential Rough Slider Bearing

8.3 Solution of the problem

Integrating the equation (8.2.2) we obtain

$$\tau_{xy} = \phi z + c_1$$

where $\phi = \frac{\partial p}{\partial x}$, c_1 is the constant of integration to be determined and ϕ is the pressure gradient in *x*-direction. Substituting in equation (2.1.1) we have

$$u = \frac{1}{4\mu}\left[2\phi y^2 + 4c_1 y + \alpha(\phi^3 y^4 + 4\phi^2 c_1 y + 6\phi c_1^2 y^2 + 4c_1^3 y)\right] + c_2 \tag{8.3.1}$$

The constants of integration, c_1 and c_2 can be determined by using the relevant boundary conditions given in equations (8.2.4) and (8.2.5). The velocity component *u* in *x*- direction is obtained as

$$u = \frac{1}{4\mu}\left[f_1 \frac{\partial p}{\partial x} + \frac{1}{2}\alpha f_2 (\phi)^3\right] + U\left\{1 - \frac{4y - \alpha f_3 (\phi)^2}{4H + \alpha H^3 (\phi)^2}\right\} \tag{8.3.2}$$

where the functions f_1, f_2 and f_3 are described by

$$f_1 = 2y^2 - 2Hy, \tag{8.3.3a}$$

$$f_2 = 2y^2 - 4Hy^3 + 3H^2 y^2 - H^3 y, \tag{8.3.3b}$$

$$f_3 = 6Hy^2 - 4y^3 - 3H^2 y. \tag{8.3.3c}$$

Integrating the continuity equation (8.2.1) across the film height under the relevant boundary conditions (8.2.4) and (8.2.5),

the modified Reynolds equation is obtained as

$$\frac{\partial}{\partial x}\left[H^3 \frac{\partial p}{\partial x} + \frac{3}{20}\alpha H^5 \left(\frac{\partial p}{\partial x} \right)^3 \right] = 6\mu U \frac{\partial H}{\partial t} . \tag{8.3.4}$$

The mathematical function for the film thickness of the considered bearings is given by

$$h(x,y) = h_2 \cdot \exp\left[-\frac{x}{L} \log\left(\frac{h_1}{h_2} \right) \right]. \tag{8.3.5}$$

In the equation (8.3.5) h_2 denotes the minimum film thickness, $d = h_1 - h_2$ is the difference between inlet and outlet film thickness.

Let the local film thickness *H* can be considered to be composed of two separate parts

$$H = h(x,y) + h(x,y,\xi) \tag{8.3.6}$$

where *h*(*x, y*) denotes the nominal smooth part of the film geometry while h_s is the part due to the surface roughness is measured from the nominal level. Without loss of generality it may be assumed that, the mean value of h_s over bearing surface is zero. The film thickness component h_s is the function of space co-ordinates *x* and *y*, and of the random variable ξ. Hence, for a given value of ξ the surface component of the film thickness becomes deterministic function of the space variables.

Let $f(h_s)$ be the probability density function of the stochastic film thickness h_s taking average of the equation (8.3.4) with respect to $f(h_s)$ we obtain

$$\frac{\partial}{\partial x}\left[E(H^3)\left(\frac{\partial E(p)}{\partial x} \right) + \frac{3}{20}\alpha E(H^5)\left(\frac{\partial E(p)}{\partial x} \right)^3 \right] = 6\mu U \frac{\partial E(H)}{\partial t} \tag{8.3.7}$$

where the expectancy operator $E(\bullet)$ is defined by

$$E(\bullet)=\int_{-\infty}^{\infty}(\bullet)f(h_s)dh_s \tag{8.3.8}$$

In accordance with the Christensen (1969-70), it is assumed that

$$f(h_s)=\begin{cases}\dfrac{35}{32c^7}(c^2-h_s^2)^3. & -c<h_s<c\\ 0 & \text{elsewhere}\end{cases} \tag{8.3.9}$$

where $\sigma=c/3$ is the standard deviation.

According to Christensen (1970) stochastic theory for the hydrodynamic lubrication of rough surfaces, the analysis is done for two types of one- dimensional surface roughness pattern viz; one-dimensional longitudinal surface roughness pattern and transverse roughness pattern. For this, equation (8.3.5) can be defined in the form

For longitudinal roughness pattern

$$\frac{\partial}{\partial x}\left[E(H^3)\left(\frac{\partial E(p)}{\partial x}\right)+\frac{3}{20}\alpha E(H^5)\left(\frac{\partial E(p)}{\partial x}\right)^3\right]=6\mu U\frac{\partial H}{\partial t}, \quad \text{and} \tag{8.3.10}$$

For transverse roughness pattern

$$\left.\begin{aligned}\frac{\partial}{\partial x}\left[\frac{1}{E\left(1/H^3\right)}\left(\frac{\partial E(p)}{\partial x}\right)+\frac{3}{20}\alpha\frac{1}{E\left(1/H^5\right)}\left(\frac{\partial E(p)}{\partial x}\right)^3\right]\\ =6\mu U\frac{\partial}{\partial t}\frac{E\left(1/H^2\right)}{E\left(1/H^3\right)}\end{aligned}\right\}. \tag{8.3.11}$$

Equations (8.3.11) and (8.3.12) together can be defined as

$$\frac{\partial}{\partial x}\left[g_1(H,c)\left(\frac{\partial E(p)}{\partial x}\right)+\frac{3}{20}\alpha g_2(H,c)\left(\frac{\partial E(p)}{\partial x}\right)^3\right]=6\mu U\frac{\partial F}{\partial t} \tag{8.3.12}$$

where

$$g(H,c)=\begin{cases} E(H). & \text{for longitudinal roughness} \\ \left[E\left(\frac{1}{H}\right)\right]^{-1} & \text{for transverse roughness} \end{cases} \tag{8.3.13a}$$

$$E(H)=\frac{35}{32c^7}\int_{-c}^{c} H(c^2-h_s^2)^3\,dh_s\ , \tag{8.3.13b}$$

$$E\left(\frac{1}{H}\right)=\frac{35}{32c^7}\int_{-c}^{c}\frac{(c^2-h_s^2)^3}{H}\,dh_s\ , \tag{8.3.13c}$$

$$F=\begin{cases} E\left(H\right) & \text{for longitudinal roughness} \\ \dfrac{E\left(1/H^2\right)}{E\left(1/H^3\right)} & \text{for transeverse roughness} \end{cases} \tag{8.3.13d}$$

To analyzing the bearing performance the following non-dimensional variables and parameters are introduced.

$$\left.\begin{aligned} &x^*=\frac{x}{L},\quad p^*=\frac{E(p)h^2}{\mu UL}\qquad \beta=\alpha\frac{\mu^2U^2}{h_2^2}, H^*=h^*+h_s\quad C=c/h_0 \\ &h^*=\frac{h}{h_2}=\exp\left(-x^*.\log(\delta+1)\right),\ \text{where}\ \ \delta=\frac{d}{h_2}\ \text{and}\ d=h_1-h_2 \end{aligned}\right\} \tag{8.3.14}$$

where $d=h_1-h_2$ the difference of inlet-outlet thickness, L is the inclined part of the bearing and $\delta=\dfrac{d}{h_2}$ is non-dimensional inlet-outlet thickness difference. β - describes the non-linear parameter of non-Newtonian fluids.

Equation (8.3.12) in non-dimensional form is

$$\frac{\partial}{\partial x^*}\left[G_1(H^*,C)\frac{\partial p^*}{\partial x^*}+\frac{3}{20}\beta G_2(H^*,C)\left(\frac{\partial p^*}{\partial x^*}\right)^3\right]=6\frac{\partial F^*}{\partial x^*} \tag{8.3.15}$$

where pressure boundary conditions are

$$p^*=0 \text{ at } x^*=-1, \text{ and } x^*=0. \tag{8.3.16}$$

The non-dimensional Reynolds equation (8.3.15) is highly non-linear ordinary differential equation. By applying small perturbation method, first order solution can be obtained

$$p^*=p_0^*+\beta p_1^*. \tag{8.3.17}$$

Substituting in to the non-linear equation and dropping higher order terms we have the zero order and first order equations respectively.

$$\frac{\partial}{\partial x^*}\left\{ G_1\left(H^*,C\right)\frac{\partial p_0^*}{\partial x^*}\right\}=6\frac{\partial F^*}{\partial x^*}, \tag{8.3.18}$$

$$\frac{\partial}{\partial x^*}\left\{ G_1\left(H^*,C\right)\frac{\partial p_1^*}{\partial x^*}+\frac{3}{20}G_2\left(H^*,C\right)\left(\frac{\partial p_0^*}{\partial x^*}\right)^3\right\}=0. \tag{8.3.19}$$

Integrating equations (8.3.18) and (8.3.19) using boundary conditions (8.3.16) expressions for pressure can be obtained as

$$p^* = \frac{6}{\eta_{B1}}\left\{\left(\eta_A.\eta_{B1}-\eta_B\eta_{A1}\right)+\frac{\beta}{40}\left(.\eta_B\eta_{C1}-\eta_C.\eta_{B1}\right)\right\} \tag{8.3.20}$$

$$\eta_A(x^*)=\int_0^{x^*}\frac{F^*}{G_1^*\left(H^*,C\right)}dx^*, \tag{8.3.21}$$

$$\eta_B(x^*)=\int_0^{x^*}\frac{1}{G_1^*\left(H^*,C\right)}dx^*, \tag{8.3.22}$$

$$\eta_C(x^*) = \int_0^{x^*} \frac{G_2^*(H^*,C)}{G_1^*\left(H^*,C\right)} \left(\frac{6\left(M^*\eta_{B1} - \eta_{A1}\right)}{G_1^*\left(H^*,C\right)\eta_{B1}} \right)^3 dx^* \quad \text{and} \tag{8.3.23}$$

$$\eta_{A1} = \eta_A\left(x^* = 1\right),\ \eta_{B1} = \eta_B\left(x^* = 1\right),\ \text{and } \eta_{C1} = \eta_C\left(x^* = 1\right).$$

Integrating the film pressure over the film pressure over the film region gives the load carrying capacity

$$W = -\int_0^{-L} p dx \quad . \tag{8.3.24}$$

The non-dimensional load carrying capacity is given by

$$W^* = \frac{Wh_2^2}{\mu U L^2} = -\int_0^{-1} p^* dx^* \tag{8.3.25}$$

$$W^* = -\int_0^{-1} \frac{6}{\eta_{B1}} \left\{ \left(\eta_{B1}\eta_A - \eta_{A1}\eta_B\right) + \frac{\beta}{40}\left(\eta_B\eta_{C1} - \eta_C\eta_{B1}\right) \right\} dx^* \tag{8.3.26}$$

$$W^* = \left[\left\{ \frac{6\left(\eta_{A1}\psi_B - \eta_{B1}\psi_A\right)}{\eta_{B1}} \right\} + \frac{162}{5} \frac{\beta}{(\eta_{B1})^3} \left\{ \frac{\eta_{B1}\psi_C - \eta_{C1}\psi_B}{\eta_{B1}} \right\} \right] \tag{8.3.27}$$

where

$$\psi_A = \int_0^{-1} \int_0^{x^*} \frac{F^*}{G_1(H^*,C)} \left(dx^*\right)\left(dx^*\right), \tag{8.3.28a}$$

$$\psi_B = \int_0^{-1} \int_0^{x^*} \frac{1}{G_1(H^*,C)} \left(dx^*\right)\left(dx^*\right) \text{ and} \tag{8.3.28b}$$

$$\psi_C = \int_0^{-1}\int_0^{x^*} \frac{G_2\left(H^*,C\right)}{G_1(H^*,C)} \left(\frac{6\left(\eta_{B1}F^* - \eta_A\right)}{\eta_{B1}G_1(H^*,C)}\right)^3 \left(dx^*\right)\left(dx^*\right) \tag{8.3.28c}$$

The friction force can be obtained by integrating the shear stress acting upon the sliding surface

$$f = -\int_{x=0}^{-L} \left(\tau_{xz}\right)_{at\ z=0} dx\ , \tag{8.3.29}$$

which is in the non-dimensional form

$$F = \frac{f_f h_2}{\mu UL} = -\int_{x^*=0}^{-1} \left\{\frac{1}{H^*} + \frac{1}{2}H^*\frac{\partial p^*}{\partial x^*} - \frac{\beta}{16}H^*\left(\frac{\partial p^*}{\partial x^*}\right)^2\right\} dx^*. \tag{8.3.30}$$

The non-dimensional coefficient of a friction C^* can be derived using

$$C^* = \frac{F}{W^*} \tag{8.3.32}$$

8.4 Results and discussion

To study the Non-Newtonian effects on the steady characteristics of rough exponential slider bearing lubricated with Rabinowitsch fluid model is analyzed. Based upon this model, the non-Newtonian properties are characterised by the non-dimensional non-linear factor β . As $\beta = 0$, the Newtonian case is recovered, for $\beta < 0$, the fluid is dilatant, for $\beta > 0$, the fluid is pseudoplastic. In the present analysis, bearing characteristics are evaluated for the following values of parameters

Profile parameter $\delta = 0.2$ to 3.0,

Non-linear factor $\beta = -0.1$ to 0.1 and

Roughness parameter $C = 0.0$ to 0.4.

If $C \to 0$ the present result is in well agreement with the smooth case. These close agreements provide a support for the present study.

Figure 8.2 shows the variation of non-dimensional pressure p^* verses x^* for different values of β with $\delta = 1.5$ and $C = 0.2$. The effect of a pseudoplastic lubricant is observed to decrease the value of p^*, but the dilatant behaviour increases the steady state film pressure. Figures 8.3 and 8.4 show the variation of non-dimensional pressure p^* verses x^* for different values of C with $\delta = 1.5$, $\beta = -0.1$ (Fig 8.3) and $\beta = 0.1$ (Fig 8.4) for both type of roughness patterns. It is observed that, p^* increases (decreases) with C in case of transverse (longitudinal) roughness parameter. Further, the roughness effects are more pronounced for the transverse roughness pattern than the longitudinal roughness pattern. The dotted curve in the graph corresponds to the longitudinal case.

The variation of non-dimensional load carrying capacity W^* with δ for different values of non-linear factor β with $C = 0.2$ for both type of roughness patterns is depicted in Figure 8.5. It is observed that, the effect of surface roughness is to increase the load carrying capacity for dilatants and decreases for pseudoplastic fluids for both types of roughness patterns. Figures 8.6 and 8.7 shows the variation of non-dimensional load carrying capacity W^* with δ for different values of C with $\beta = -0.1$ (Fig 8.6) and $\beta = 0.1$ (Fig 8.7). It is observed that, the load carrying capacity increases (decreases) with C in case of transverse (longitudinal) roughness pattern. Further, it is observed that, the roughness effects are more pronounced for transverse roughness pattern than the longitudinal roughness pattern. . Further it is also observed that, load carrying capacity is more for the dilatant lubricant as compared with the pseudoplastic fluids.

Figure 8.8 shows that variation of frictional force with respect to the profile parameter δ for different non-linear factor β with C = 0.2. It is observed that frictional force decreases as δ increases. The variation of frictional force with respect to the profile parameter δ for different C is depicted in Figure 8.9 ($\beta = -0.1$) and in Figure 8.10 ($\beta = 0.1$) for both types of roughness patterns. It is observed that, there is decrease in the in frictional force as δ increases. Further, it is also observed that, more frictional force is for dilatant lubricants as compared with the pseudoplastic lubricants. If C = 0 results are well agreement with smooth case.

Figure 8.11 depicts the variation of coefficient of friction C^* with respect to profile parameter δ for different values of β with C = 0.2. The coefficient of friction is observed to decrease with increase in the profile parameter δ . Also for each value of δ , the coefficient of friction for $\beta = -0.1$ is smaller than that for $\beta = 0$ (Newtonian case), but for $\beta = 0.1$, it is higher than Newtonian case. Therefore, on comparison with Newtonian case, the dilatant fluids decreases the coefficient of friction and hence enhances the load carrying capacity, whereas pseudoplaticity increases the values of coefficient of friction C^* and decreases the load carrying capacity shows in the Figure 8.5. Figures (8.12-8.13) shows the variation of coefficient of friction C^* with respect to profile parameter δ for different values of C with $\beta = -0.1$ and $\beta = 0.1$. For both dilatant and pseudoplastic lubricants it is observed that there is decrease in coefficient of friction as profile parameter increases and C^* is higher for pseudoplastic lubricants as compared with the dilatant lubricants. Further, it is also observed, that as roughness parameter increases coefficient of friction decreases.

C^* is higher in case of longitudinal roughness pattern in both pseudoplastic lubricants and dilatant lubricants.

8.5 Conclusion

On the basis of Christensen (1973) stochastic theory for hydrodynamic lubrication of rough surfaces, the effect of surface roughness on static characteristics of exponential slider bearing lubricated with Rabinowitsch fluid is studied. On the basis of numerical computations of the results obtained, the following conclusions are drawn.

1. The load carrying capacity decrease for increasing values of β for both types of roughness patterns i.e. the load carrying capacity for dilatant lubricants is higher than pseudoplastic lubricants.
2. Pressure increases as β decreases from 0.1 to - 0.1
3. As roughness parameter increases both pressure and load carrying capacity increases (decreases) for transverse (longitudinal) roughness patterns.
4. The steady state load capacity increase with δ up to $\delta \approx 1.3$ and decreases thereafter.
5. The results are well agreement with the smooth case.

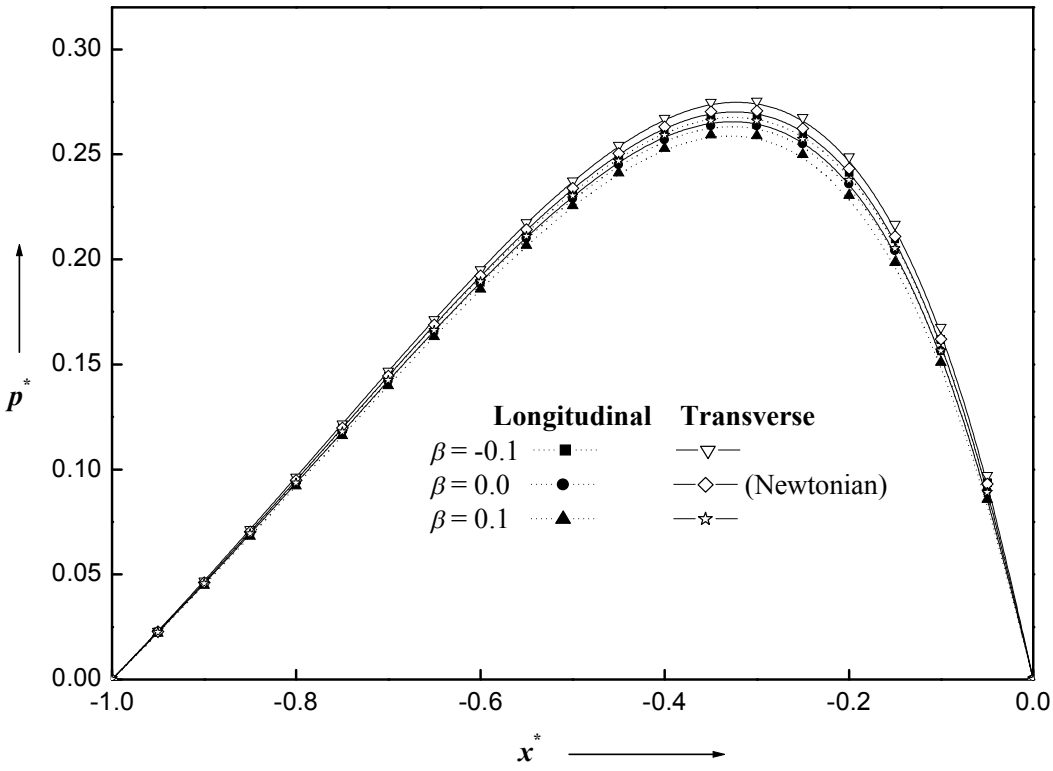

Figure 8.2 Variation of non-dimensional pressure p^* with x^* for different values of β with $\delta = 1.5$ and $C = 0.2$.

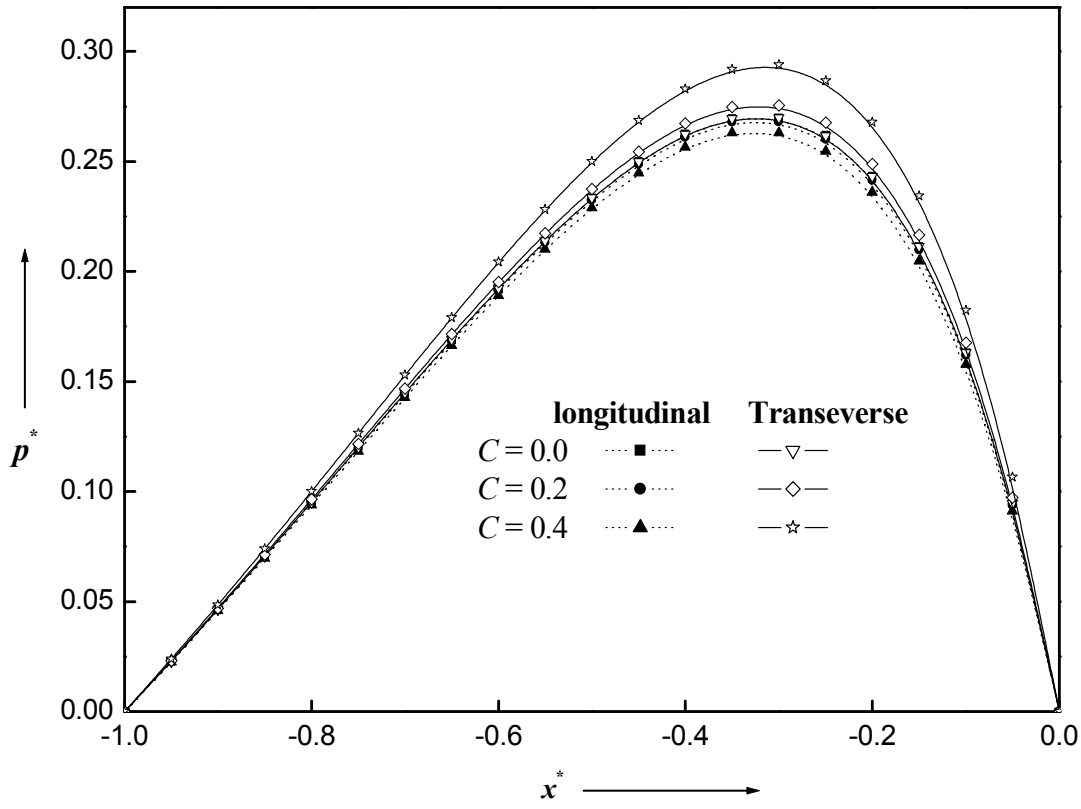

Figure 8.3 Variation of non-dimensional pressure p^* with x^* for different values of C with $\delta = 1.5$ and $\beta = -0.1$

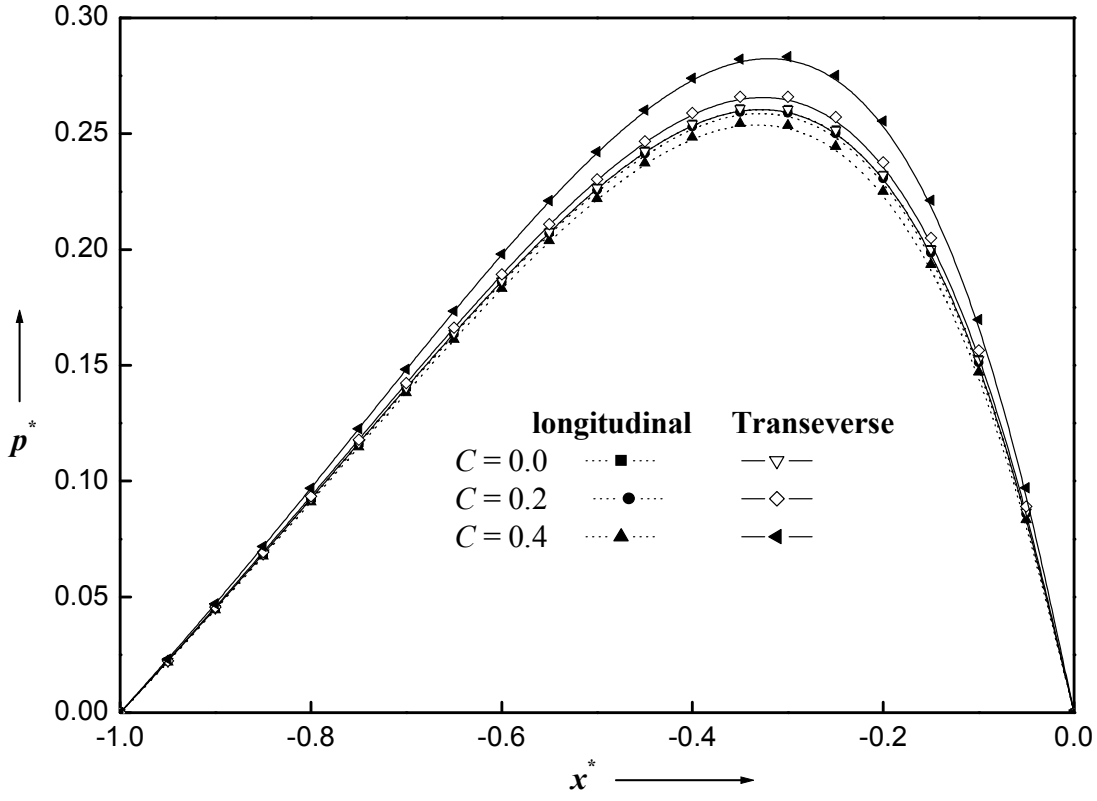

Figure 8.4 Variation of non-dimensional pressure p^* with x^* for different values of C with $\delta = 1.5$ and $\beta = 0.1$

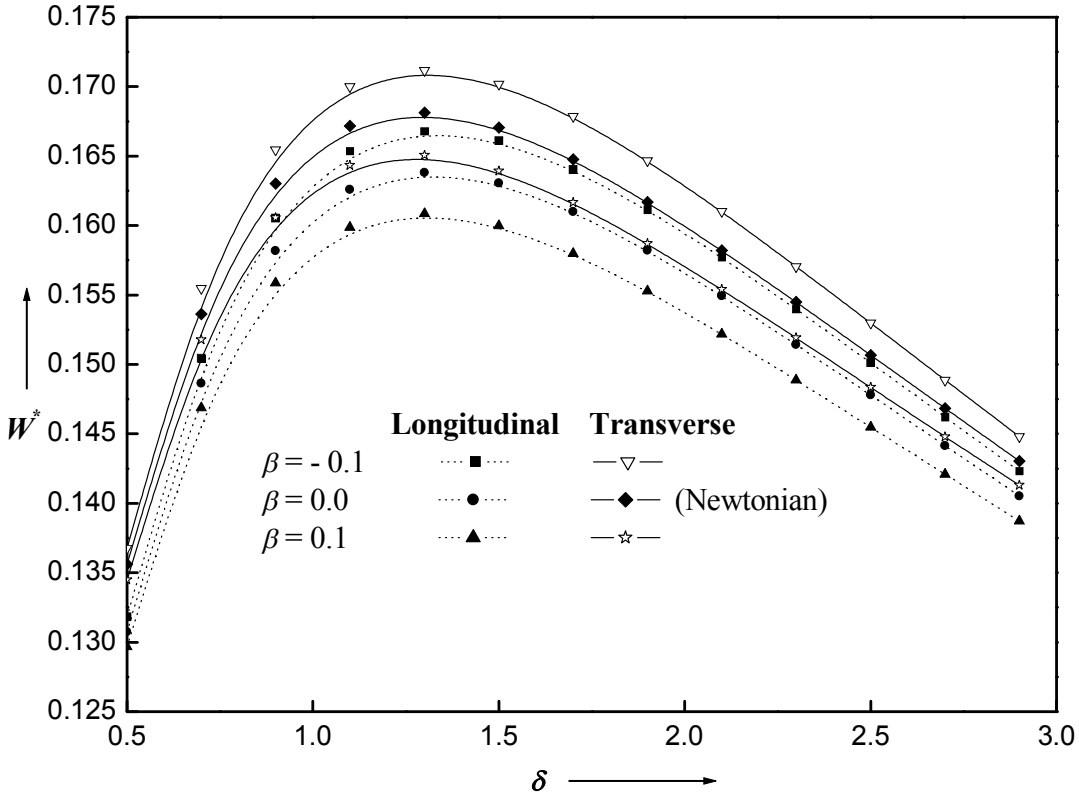

Figure 8.5 Variation of non-dimensional load carrying capacity W^* with δ for different values of β with $C = 0.2$.

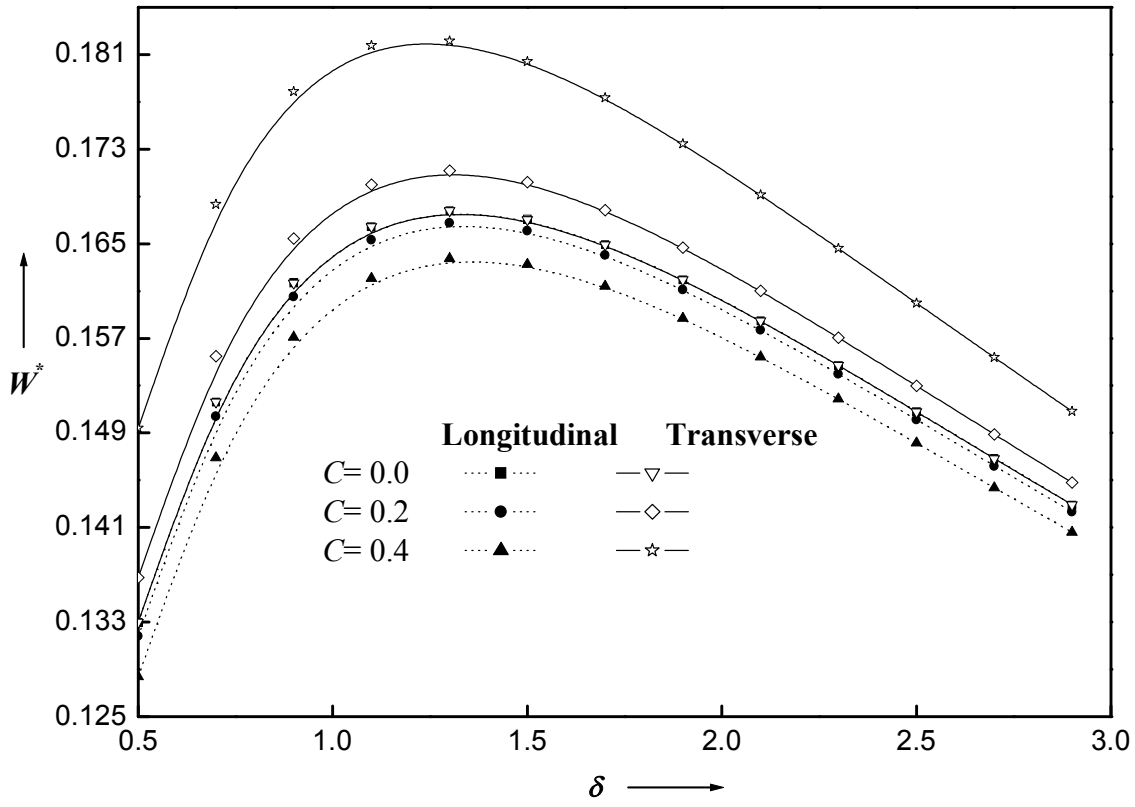

Figure 8.6 Variation of non-dimensional load carrying capacity W^* with δ for different values of C with $\beta = -0.1$.

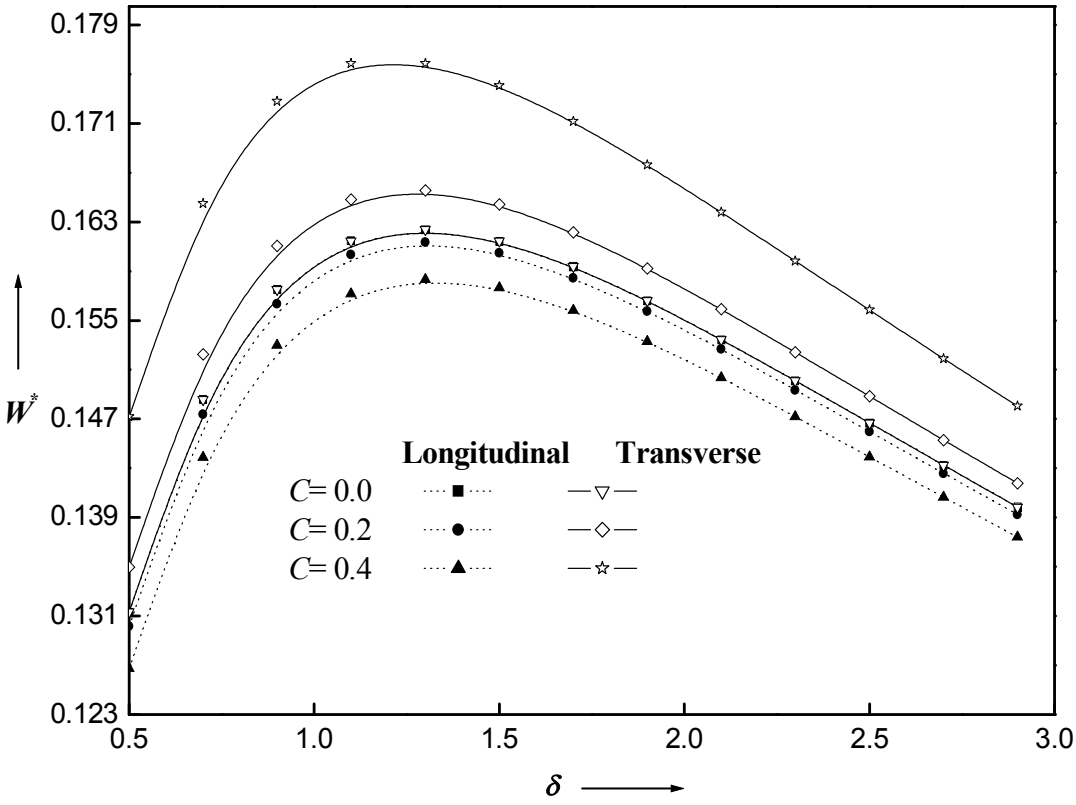

Figure 8.7 Variation of non-dimensional load carrying capacity W^* with δ for different values of C with $\beta = 0.1$.

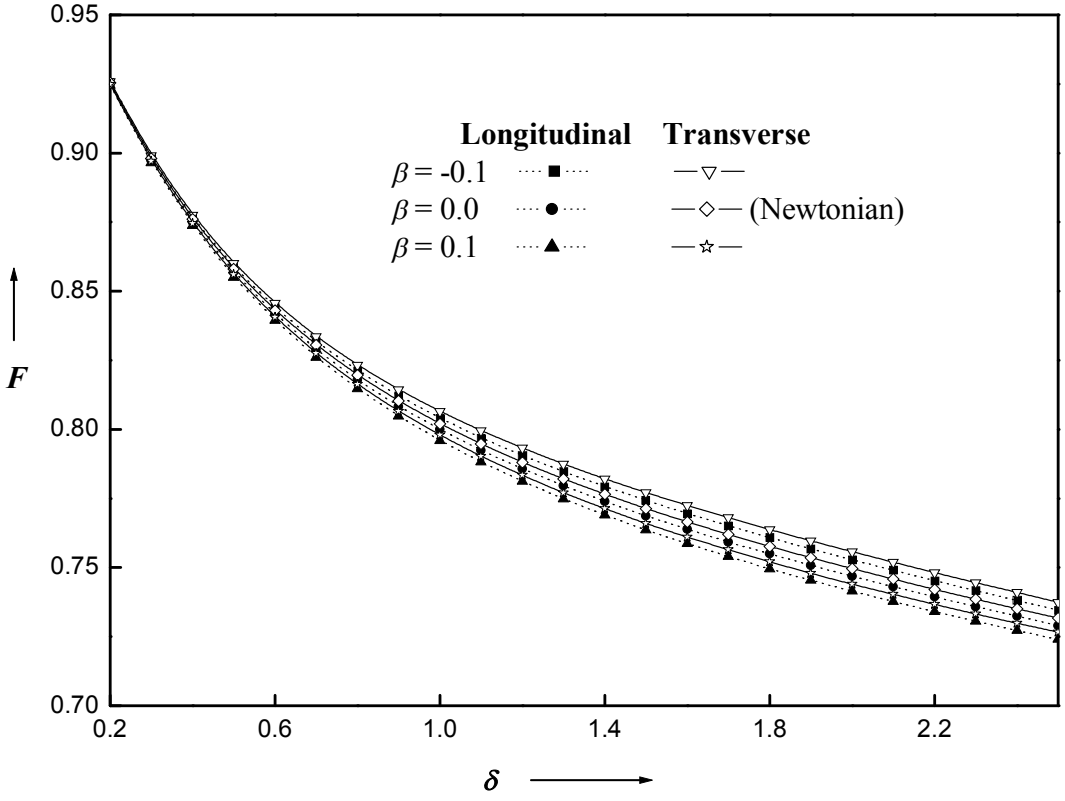

Figure 8.8 Frictional force F with profile parameter δ for different values of β with $C = 0.2$

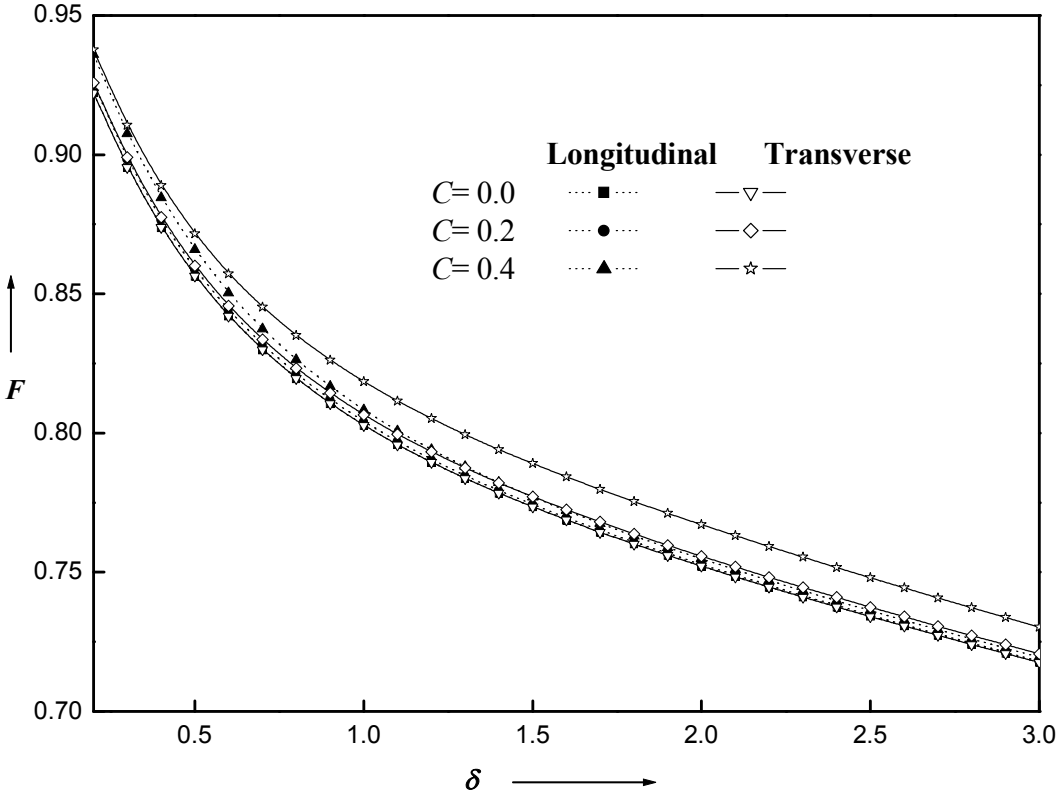

Figure 8.9 Frictional force F verses profile parameter δ for different C with $\beta = -0.1$

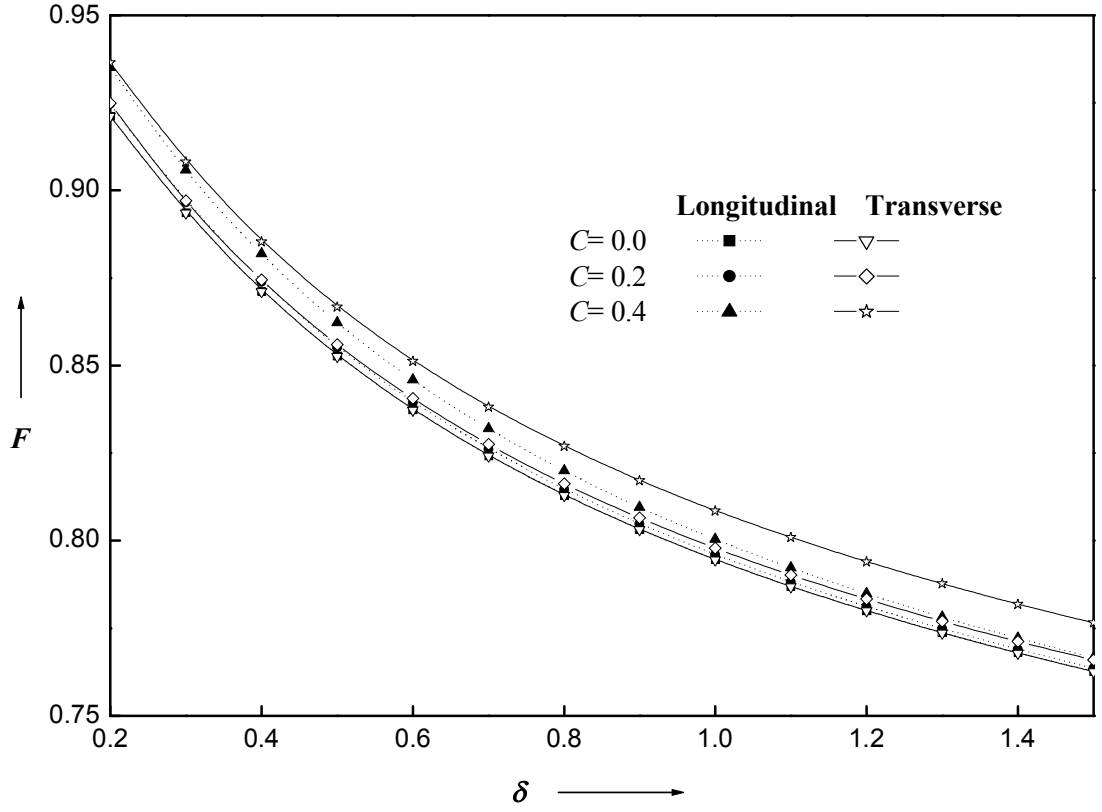

Figure 8.10 Frictional force F verses profile parameter δ for different C with $\beta = 0.1$

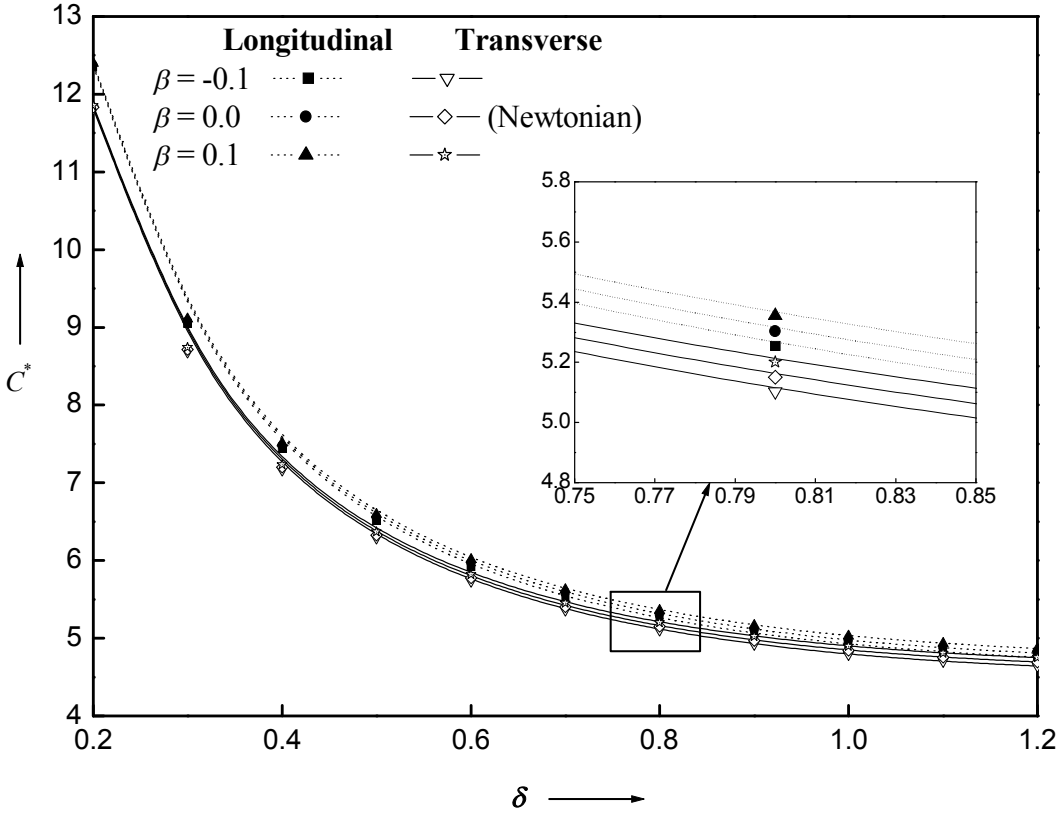

Figure 8.11 Variation of coefficient of friction C^* verses profile parameter δ for different values of β with $C = 0.2$.

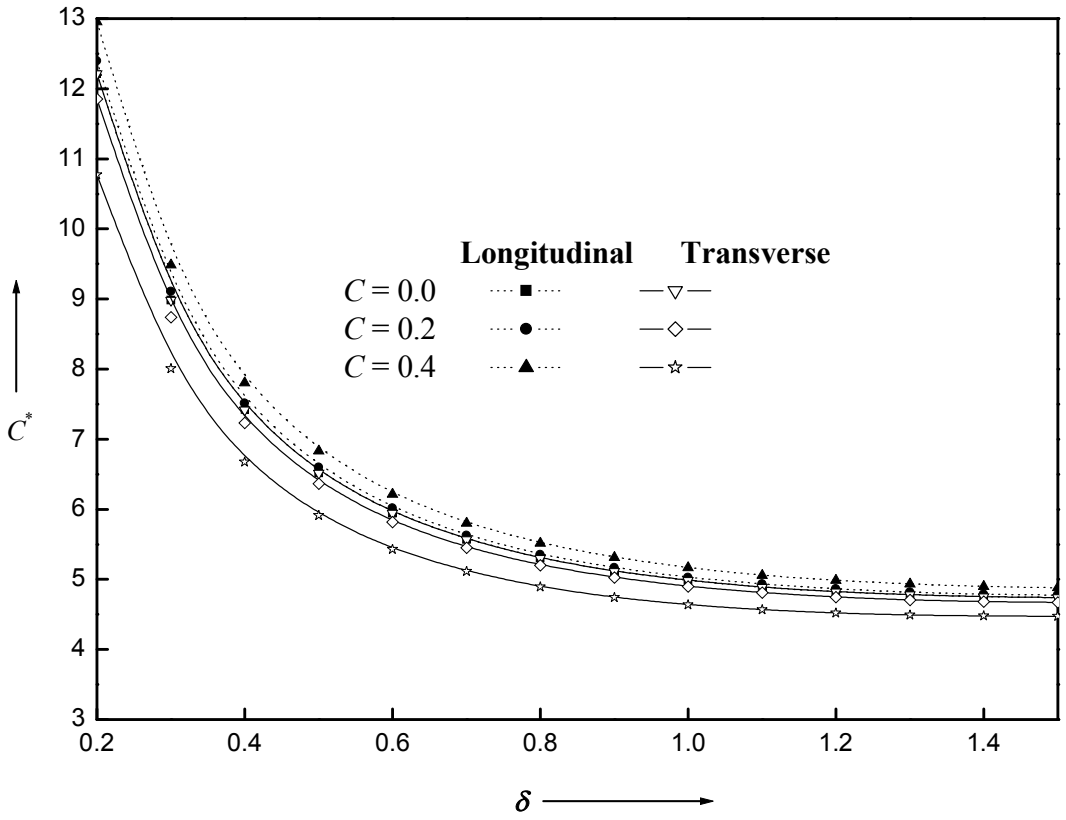

Figure 8.12 Variation of coefficient of friction C^* verses profile parameter δ for different values of C with $\beta = 0.1$

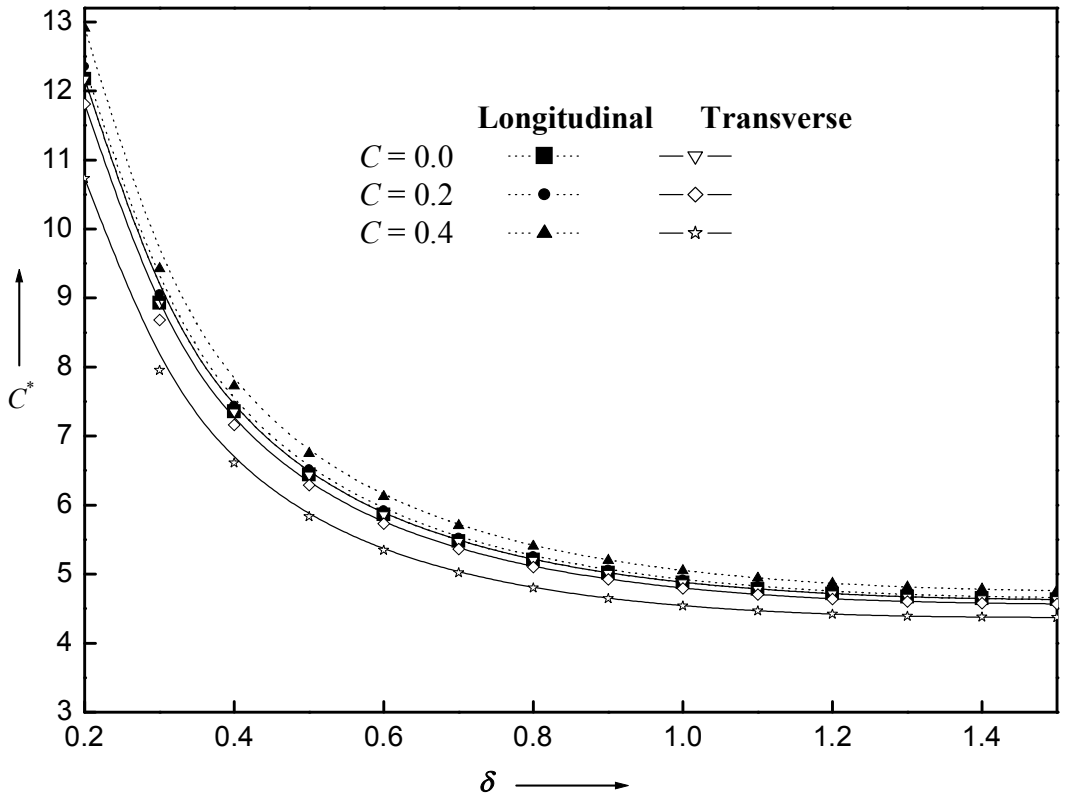

Figure 8.13 Variation of coefficient of friction C^* verses profile parameter δ for different values of C with $\beta = -0.1$